



PUBLISHED FOR SISSA BY SPRINGER

RECEIVED: December 17, 2010

ACCEPTED: February 7, 2011

PUBLISHED: February 24, 2011

Simple and realistic composite Higgs models in flat extra dimensions

Giuliano Panico,^a Mahmoud Safari^b and Marco Serone^{b,c}

^a*Institute for Theoretical Physics, ETH Zurich,
8093 Zurich, Switzerland*

^b*International School for Advanced Studies (SISSA) and
Istituto Nazionale di Fisica Nucleare (INFN),
Via Bonomea 265, I-34136 Trieste, Italy*

^c*Abdus Salam International Center for Theoretical Physics (ICTP),
Strada Costiera 11, I-34151 Trieste, Italy*

E-mail: panico@phys.ethz.ch, safari@sisssa.it, serone@sisssa.it

ABSTRACT: We construct new composite Higgs/gauge-Higgs unification (GHU) models in flat space that overcome all the difficulties found in the past in attempting to construct models of this sort. The key ingredient is the introduction of large boundary kinetic terms for gauge (and fermion) fields. We focus our analysis on the electroweak symmetry breaking pattern and the electroweak precision tests and show how both are compatible with each other. Our models can be seen as effective TeV descriptions of analogue warped models. We point out that, as far as electroweak TeV scale physics is concerned, one can rely on simple and more flexible flat space models rather than considering their unavoidably more complicated warped space counterparts. The generic collider signatures of our models are essentially undistinguishable from those expected from composite Higgs/warped GHU models, namely a light Higgs, colored fermion resonances below the TeV scale and sizable deviations to the Higgs and top coupling.

KEYWORDS: Beyond Standard Model, Field Theories in Higher Dimensions

ARXIV EPRINT: [1012.2875](https://arxiv.org/abs/1012.2875)

Contents

1	Introduction	1
2	General framework	4
3	Model I: FBKT₁₀	8
3.1	Results	12
4	Model II: FBKT₅	13
4.1	Results	16
5	Model III: modified MCHM₅	16
5.1	Results	19
6	Comments on the EWPT	20
7	Conclusions	21
A	One-loop fermion contribution to the S, T parameters and the $Zb_L\bar{b}_L$ vertex	22
A.1	Singlet with $Y = 2/3$	22
A.2	Doublet with $Y = 1/6$	23
A.3	Doublet with $Y = 7/6$	24
A.4	Triplet with $Y = 2/3$	24
A.5	Doublet with $Y = 7/6$ mixing with singlet with $Y = 5/3$	25

1 Introduction

Many alternative scenarios of new physics beyond the Standard Model (SM) have been proposed to address the gauge hierarchy problem. Among these, an intriguing idea is the possibility of identifying the Higgs field with the internal component of a gauge field in extra dimensions [1–7], resulting in the so called gauge-Higgs unification (GHU) models. In warped space [8, 9], as suggested by the AdS/CFT duality, GHU models can be seen as a (relatively) weakly coupled 5D dual of 4D strongly coupled conformal field theories [10–12], where the Higgs field emerges as a composite pseudo-Goldstone bound state of the strong sector [13, 14].¹ From a wider perspective, GHU models in warped space are concrete and

¹Contrary to the original AdS/CFT duality [15–17], where both sides of the duality are well-defined, the 4D dual theories of the GHU models in warped spaces are unknown. More precisely, what is so far lacking is an UV description of the 4D theories in terms of fundamental states such as quarks, gluons or strings, while we know, through the 5D construction, the low-energy “chiral” Lagrangian associated to them.

successful realizations of the old idea [18, 19] of composite Higgs models. The simplest composite Higgs models consist of two sectors: an “elementary” sector, which includes the gauge and fermion fields of the Standard Model (SM), and a “composite” sector, which is strongly coupled and is invariant under a suitable global symmetry. The dynamics of the composite sector induces a spontaneous breaking of the global symmetry, giving rise to a set of Goldstone bosons, that, for a judicious choice of the symmetry group, can be identified with the Higgs field. A small explicit breaking of the global symmetry is induced by gauging a part of it via the SM gauge bosons and by the weak mixing of the SM fermions with the strong sector. The composite Higgs is thus a pseudo-Goldstone boson and acquires a potential at the radiative level, which triggers electroweak symmetry breaking.

The symmetry structure of the composite Higgs scenario can be efficiently used to perform some model-independent studies by using purely 4D low-energy effective field theory considerations. This approach has been followed to find general parametrizations of the non-linear sigma model describing the Higgs field and its interactions [20] and of the interplay of the SM fermions of the elementary sector with the composite sector [21].

Despite the importance of understanding general qualitative properties of composite Higgs models by means of 4D effective field theory methods, these approaches can not furnish a complete description of the composite Higgs scenario. In particular, they do not allow to study all the properties of the strongly coupled sector and they do not allow to compute quantities which are related to a UV completion of the effective theory. A more quantitative description of the composite Higgs scenario is so far only possible by constructing explicit GHU models in extra dimensions. These allow to extract all the relevant low-energy observables, including the ones which are usually not computable in the 4D theories, namely the Higgs potential and the detailed mass spectrum of the theory, which is a crucial ingredient in determining the electroweak precision parameters. The symmetries of the extra dimensional set-up can be made explicit by using a holographic effective description [22–25], in which the “elementary” sector of the composite Higgs models is identified with the field components localized at one end-point of the extra-dimension (hereafter denoted UV brane), taken to be a segment, and the “composite” sector is identified with the remaining field components in the bulk. In this way, it is manifest that the Higgs field can be equivalently seen as a set of pseudo-Goldstone bosons coming from a spontaneous breaking of the extra dimensional gauge invariance and that the theory in the low-energy regime reproduces the symmetry structure of the SM.

Constructing a realistic composite Higgs/GHU model is not an easy task. The most constraining electroweak bounds one should consider are given by the T and S parameters [26, 27] and by the deviation δg_b with respect to the SM value of the coupling between the left-handed (LH) bottom quark and the Z vector boson. Couplings $g_{bt,R}$ between the right-handed (RH) top and bottom quarks with the W^\pm vector bosons should also be taken into account, given the rather stringent experimental bounds on them of $\mathcal{O}(10^{-3})$ [28]. Potentially deadly tree-level corrections to T and δg_b can be controlled by appropriate custodial symmetries [29, 30], but some tension with the experimental bounds still remains due to sizable one-loop corrections to T and δg_b coming from the fermion sector of these theories [31, 32]. Studying composite Higgs/GHU models in warped space is also not tech-

nically easy. As a matter of fact, although a few 5D GHU models have been constructed so far [14, 33, 34], only in one model [35] (a modified version of a model introduced in [33] to accommodate a Dark Matter candidate) one-loop corrections to S , T and δg_b (and the Higgs potential explicitly determined) have been analyzed and the ElectroWeak Precision Tests (EWPT) successfully passed. It is then important to look for other potentially interesting models and possibly find different phenomenological features of the composite Higgs scenario.

In the present work we want to point out that, as far as we are interested in the low-energy phenomenology of the composite Higgs models, we do not really need to consider the technically challenging warped models. Instead, we can rely on the much simpler flat space implementations of the GHU idea. The resulting models may still be reinterpreted as calculable 5D descriptions of 4D strongly coupled composite Higgs models. This is guaranteed by the holographic interpretation, which shows that the low-energy symmetries of the theory are independent of the specific form of the 5D metric. The Goldstone nature of the Higgs fields, as well as the phenomenology of the fermionic and gauge sectors, are similar on flat and warped spaces. We can also identify, through the 5D description, the low-energy “chiral” Lagrangian associated to a would-be strongly coupled 4D dual theory. The only relevant ingredient that warped space adds to this view is the near-conformality of the 4D strong sector. This is an important feature for what concerns the high-energy running of the parameters of the theory and the generation of a hierarchy between the electroweak scale and some high-energy scale, such as the Planck mass. However, as far as electroweak symmetry breaking dynamics and collider phenomenology is concerned, these high-energy properties are not essential and can be reliably omitted from an effective description.

Unfortunately, the simplest constructions of GHU models in flat space (see [36] for an overview and for earlier references) turned out to be not fully satisfactory (see e.g. [37, 38]). One of the reasons for this failure was the lack of some custodial protection mechanism for the electroweak precision parameters. If custodial symmetries are introduced, the situation improves but this is still not enough to build realistic theories, since one gets too low top and Higgs masses. Another key ingredient are the so called boundary kinetic terms (BKT) [39]. When these are introduced and taken to be large, potentially realistic models can be constructed.² More in detail, we construct in this paper three different models, all based on the minimal gauge group $SO(5) \times U(1)_X$, with bulk fermions in the fundamental or adjoint representation of $SO(5)$. In all the models, large BKT at the UV brane for the gauge fields are introduced. In two models, large BKT at the UV brane for the bulk fermions are also assumed. We denote them FBKT₁₀ and FBKT₅ models, where 5 and 10 denote the $SO(5)$ representations of the fermion bulk multiplets. In the third and last model no fermion BKT are introduced. This model is actually not new, but rather a flat space adaptation [36] of a model introduced in [33]. We denote it with the same acronym used in [33], MCHM₅. All the models successfully pass the EWPT, as can be seen in

²The potential interest of large BKT were already appreciated in [40], but applied to a model with $SU(3)$ gauge group, where the absence of a custodial symmetry led to large tree-level corrections to the T parameter. The possibility of getting realistic flat space models with $SO(5)$ gauge group and large BKT was recently pointed out in [36].

figures 1, 4 and 7. As far as naturalness is concerned, the MCHM₅ model is the one with the best performances, with a fine-tuning roughly estimated at the 10% level. This is around a few % in the FBKT₁₀ and FBKT₅ models. The LH top and bottom doublet and the RH top quark show a sizable degree of compositeness in all models. Considering flat space leads to a great technical simplification in model building and to very explicit and significantly simpler expressions for various quantities compared to the warped space case. Moreover, the number of free parameters can be reduced and the fermion multiplet structure in 5D can be simplified.

The structure of the paper is as follows. In section 2 we present the general framework underlying all our models and the procedure used to compute the EWPT. In sections 3, 4 and 5 we introduce respectively the FBKT₁₀, FBKT₅ and MCHM₅ models and the corresponding results. In section 6 we conclude. We report in appendix A some simple analytic formulas for the one-loop fermion contributions to T , S and δg_b that might help the reader to understand how the EWPT are successfully passed in our models.

2 General framework

All the models we consider in this paper share some common properties that are summarized below. The bulk gauge group is taken to be $G = \text{SU}(3)_c \times \text{SO}(5) \times \text{U}(1)_X$. As well-known, $\text{SO}(5)$ is the smallest group containing an $\text{SU}(2)$ custodial symmetry and giving rise to only one Higgs doublet. The subgroup $\text{U}(1)_X$ is necessary to reproduce the correct weak-mixing angle. We denote by g_5 and g_{5X} the 5D gauge coupling constants of $\text{SO}(5)$ and $\text{U}(1)_X$, respectively. The unbroken group at $y = L$ is $H = \text{SU}(3)_c \times \text{SO}(4) \times \text{U}(1)_X \simeq \text{SU}(3)_c \times \text{SU}(2)_L \times \text{SU}(2)_R \times \text{U}(1)_X$. The unbroken group at $y = 0$ is $H' = \text{SU}(3)_c \times \text{SU}(2)_L \times \text{U}(1)_Y = G_{SM}$, where the hypercharge Y is $Y = X + T_{3R}$.

We work in the following in the “holographic” basis for the gauge fields, namely we define the SM gauge fields as those which have SM couplings (with no deviations) to the elementary fermions (i.e. completely localized at $y = 0$ [23]). We use holographic techniques to efficiently compute the Higgs potential and tree-level corrections to electroweak observables (see [36] for an introduction to the basic holographic techniques used in models with extra dimensions). In the “holographic” unitary gauge $A_y = 0$ [25], the Higgs field is encoded in the sigma-model field (see appendix C of [36] for our $\text{SO}(5)$ conventions):

$$\Sigma = \exp \left[\sum_{\hat{a}=1}^4 i \frac{\sqrt{2} t^{\hat{a}} h_{\hat{a}}}{f_{\pi}} \right], \quad f_{\pi} = \frac{\sqrt{2}}{g_5 \sqrt{L}}. \quad (2.1)$$

Neglecting the color $\text{SU}(3)_c$ factor, the boundary conditions (b.c.) for the (non-canonically normalized) gauge fields are as follows:

$$\begin{aligned} F_{\mu y, L}^a &= F_{\mu y, R}^a = F_{\mu y, X} = 0, \quad A_{\mu}^{\hat{a}} = 0, \quad a = 1, 2, 3, \hat{a} \in \mathcal{G}/\mathcal{H}, \quad y = L, \\ F_{\mu y, L}^a &= F_{\mu y, R}^3 + F_{\mu y, X} = 0, \quad A_{\mu}^{\hat{a}} = A_{\mu, R}^{1,2} = 0, \quad A_{\mu, R}^3 = A_{\mu, X} = B_{\mu}, \quad y = 0. \end{aligned} \quad (2.2)$$

We introduce localized gauge kinetic terms at $y = 0$ only. The EW gauge Lagrangian is

$$\mathcal{L}_g = \mathcal{L}_{5g} + \mathcal{L}_{4g,0} + \mathcal{L}_{4g,L}, \quad (2.3)$$

with

$$\begin{aligned} \mathcal{L}_{5g} &= \int_0^L dy \left\{ \frac{1}{2g_5^2} \text{Tr} \left[-\frac{1}{2} F_{\mu\nu}^2 + (\partial_y A_\mu)^2 \right] + \frac{1}{2g_{5X}^2} \left[-\frac{1}{2} F_{\mu\nu,X}^2 + (\partial_y A_{\mu,X})^2 \right] \right\}. \\ \mathcal{L}_{4g,0} &= -\frac{\theta L}{4g_5^2} \sum_{a=1}^3 (W_{\mu\nu}^a)^2 - \frac{\theta' L}{4g_{5X}^2} B_{\mu\nu}^2, \quad \mathcal{L}_{4g,L} = 0. \end{aligned} \quad (2.4)$$

In eq. (2.4), $W_{\mu\nu}$ and $B_{\mu\nu}$ are the field strengths of the $SU(2)_L$ and $U(1)_Y$ gauge bosons, respectively, θ and θ' are dimensionless parameters and the $SO(5)$ generators are normalized as $\text{Tr} t_a t_b = \delta_{ab}$ in the fundamental representation. We do not report the holographic Lagrangian for the SM gauge fields W_μ^a and B_μ , that can be found in [36]. The SM gauge couplings constants g , g' , and the Higgs VEV v are related as follows to the 5D parameters:

$$\frac{1}{g^2} \simeq \frac{L(1+\theta)}{g_5^2}, \quad \frac{1}{g'^2} \simeq \frac{L(1+\theta')}{g_{5X}^2} + \frac{L}{g_5^2}, \quad v^2 = \frac{2s_\alpha^2}{g_5^2 L} = f_\pi^2 s_\alpha^2, \quad (2.5)$$

valid for $\alpha \lesssim 1/3$, the region of interest. In eq. (2.5),

$$s_\alpha \equiv \sin(\alpha), \quad \alpha = \frac{\langle h \rangle}{f_h}, \quad h = \sqrt{\sum_{\hat{a}=1}^4 h_{\hat{a}}^2}, \quad \langle h \rangle \simeq 246 \text{ GeV}. \quad (2.6)$$

In the holographic basis, the custodial $SU(2)_D$ symmetry, unbroken at $y = L$, is completely manifest, resulting in a vanishing T parameter at tree-level [29]. The S parameter is not vanishing and given by

$$S_{\text{tree}} \simeq \frac{4s_W^2}{3\alpha_{em}} \frac{s_\alpha^2}{1+\theta}, \quad (2.7)$$

where α_{em} is the electromagnetic constant at the M_Z scale, $\alpha_{em} \simeq 1/129$, and $s_W \equiv \sin \theta_W$, with θ_W the weak-mixing angle. For $s_\alpha \lesssim 1/3$, the mass of the W is given by

$$M_W \simeq \frac{s_\alpha}{\sqrt{2}L\sqrt{\theta+1}}. \quad (2.8)$$

In the same limit, the mass M_g of the lightest non-SM vector mesons is

$$M_g \simeq \frac{\pi}{2L}. \quad (2.9)$$

The gauge contribution to the Higgs potential, for $\theta \sim \theta' \gg 1$ and $s_\alpha \ll 1$, is well approximated by

$$V_g \simeq \frac{3}{2} \int \frac{d^4 p}{(2\pi)^4} \left[2 \log \left(1 + s_\alpha^2 \frac{\Pi_g^- - \Pi_g^+}{2(\Pi_g^+ + \theta L p^2)} \right) + \log \left(1 + s_\alpha^2 \frac{\sec^2 \theta_W (\Pi_g^- - \Pi_g^+)}{2(\Pi_g^+ + \theta L p^2)} \right) \right], \quad (2.10)$$

where

$$\Pi_g^+(p) = p \tan(pL), \quad \Pi_g^-(p) = -p \cot(pL). \quad (2.11)$$

Let us now turn to the model-dependent fermion sector of the Lagrangian. We only consider bulk fermions in the **5** or **10** representation of $SO(5)$. The fermion Lagrangian that encompasses all models has the following form:

$$\mathcal{L}_f = \mathcal{L}_{5f} + \mathcal{L}_{4f,0} + \mathcal{L}_{4f,L}, \quad (2.12)$$

with

$$\mathcal{L}_{5f} = \int_0^L dy \left[\sum_{i=1}^{n_5} \bar{\xi}_i (i\not{D} - m_i) \xi_i + \sum_{\alpha=1}^{n_{10}} \text{Tr} \bar{\xi}_\alpha (i\not{D} - m_\alpha) \xi_\alpha \right], \quad (2.13)$$

$$\mathcal{L}_{4f,0} = \sum_n Z_n \bar{\psi}_n i\not{D} \psi_n, \quad (2.14)$$

$$\mathcal{L}_{4f,L} = \sum_n \tilde{m}_n \bar{\psi}_n \tilde{\psi}_n + h.c.. \quad (2.15)$$

In eq. (2.13) ξ_i and ξ_α denote the bulk fermions in the **5** and **10** of SO(5), respectively. In eq. (2.14) ψ_n denote the $SU(2)_L \times U(1)_Y$ chiral fermion components of the bulk multiplets that are not vanishing at $y = 0$, and Z_n are their corresponding boundary kinetic terms. In eq. (2.15) ψ_n and $\tilde{\psi}_n$ denote the $SO(4) \times U(1)_X$ chiral fermion components of the bulk multiplets that are not vanishing at $y = L$ and can mix through the mass terms \tilde{m}_n . The fermions ψ_n and $\tilde{\psi}_n$ have classical dimension two in mass, like a 5D fermion, so that the BKT Z_n have dimension one and the IR mass terms \tilde{m}_n are dimensionless. No localized fermions are introduced.

Once the symmetry between the two-end points $y = 0$ and $y = L$ is broken by the BKT, the end-point (UV brane) where the BKT are non-vanishing effectively defines the “elementary” sector of the composite Higgs model and the resulting models resemble more closely the analogue ones in warped space. This is the main reason why we have not introduced similar BKT at $y = L$ for gauge and fermion fields. This choice is quantum mechanically stable. If not introduced at a given scale, BKT at $y = L$ will appear through running effects [41], but with small coefficients $\sim g^2/(16\pi^2)$. Large BKT are also quantum mechanically stable, since in the limit in which the BKT becomes infinite, the zero mode of the Kaluza-Klein (KK) tower of the associated field becomes purely elementary and decouples from the massive composite KK modes.³ Including large BKT for the fermions is thus natural and does not affect the cut-off Λ of the model. On the contrary, the gauge BKT have an impact on Λ and tend to lower it (for a discussion see e.g. [36]). The difference with the fermions comes from the fact that the gauge BKT determine the 4D gauge coupling constant. If we fix the 4D gauge coupling, in order to obtain large values for the θ parameters we need to increase the 5D gauge coupling, thus lowering Λ .

As mentioned in the introduction, the most stringent bounds on 5D models of this sort come from the S and T parameters and by the deviation δg_b to the $Z b_L \bar{b}_L$ coupling. In all our models we exploit the \mathbf{Z}_2 LR symmetry that allows to keep the tree-level correction to δg_b under control [30]. We compute the latter by using the holographic approach. The main contribution to δg_b arises from higher order operators with Higgs insertions, which give a contribution of $\mathcal{O}(\alpha^2)$. Higher-order derivative operators are suppressed by the fermion masses or Z boson masses and are respectively $\mathcal{O}(m_b L)^2$ or $\mathcal{O}(m_Z L)^2 \sim \mathcal{O}(\alpha^2/\theta)$, where eq. (2.8) has been used in the latter relation. For large BKT, $\theta \gg 1$, all higher derivative operators can be neglected and we can reliably set the momentum of all external fields to

³This can be easily seen by noticing that the shape of the zero-mode wave function is independent of the BKT and, in the limit of infinite BKT, its normalization goes to zero.

zero. In this limit, the computation greatly simplifies and compact analytic formulas can be derived.

Since the symmetries protecting the T parameter and $Zb_L\bar{b}_L$ at tree-level are not exact, one-loop effects to such observables are expected to be important and must be included [31, 32]. Non-SM fermions, being significantly lighter than non-SM vector mesons, play the dominant role, so it is a good approximation to just compute the one-loop fermion (top) contribution to T and δg_b .⁴ Performing one-loop computation using holographic techniques is not easy, so we resort here to the more standard KK approach. Along the lines of [31, 32], we compute the masses and the Yukawa couplings mixing the lightest KK states with the top quark and by standard techniques compute the one-loop correction to T and δg_b [42]. We actually also compute one-loop corrections to S ,⁵ since the one-loop suppression factor $g^2/(16\pi^2)$ is partially compensated by the mild hierarchy between the masses of the lightest non-SM gauge and fermion states. Indeed, the one-loop contribution to S given by a fermion (see appendix) is roughly $\mathcal{O}(N_c y^2 v^2 / (4\pi M_f^2))$, where y is a Yukawa coupling, M_f a vector-like fermion mass and $N_c = 3$ is the QCD color factor. Using eqs. (2.8) and (2.9), we can write the ratio between the one-loop and the tree-level correction to S as follows:

$$\frac{S_{1-loop}}{S_{tree}} \sim \frac{N_c y^2 M_g^2}{16\pi^2 M_f^2}. \quad (2.16)$$

Given that typically $M_g^2 \gtrsim 10M_f^2$, we see that one-loop corrections to S cannot totally be ignored, although they play a sub-dominant role with respect to T and δg_b .⁶ We report in appendix A analytic formulas for the new physics fermion contribution to S , T and δg_b in the simplified case in which only one vector-like fermion ($SU(2)_L$ singlet, doublet or triplet) is relevant.

Possibly dangerous $Wb_R\bar{t}_R$ couplings are generated at tree-level only in the FBKT₁₀ model. In contrast to δg_b , one-loop corrections to $g_{bt,R}$ are expected to be negligible, being suppressed by the small bottom Yukawa coupling.

We test our models by performing a combined χ^2 fit expressed in terms of the ϵ_i parameters [43–45], following [46]. We use the following theoretical values for the ϵ_i parameters⁷

$$\begin{aligned} \epsilon_1 &= (5.64 - 0.86 lh) \times 10^{-3} + \alpha_{em} T_{NP}, \\ \epsilon_2 &= (-7.10 + 0.16 lh) \times 10^{-3}, \\ \epsilon_3 &= (5.25 + 0.54 lh) \times 10^{-3} + \frac{\alpha_{em}}{4 \sin^2 \theta_W} S_{NP}, \\ \epsilon_b &= -6.47 \times 10^{-3} - 2\delta g_{b,NP}, \end{aligned} \quad (2.17)$$

⁴In the holographic basis of the gauge fields, $Zb_L\bar{b}_L$ has anyhow only fermion contributions, since the mixing in the gauge sector (i.e. the S-parameter) is rotated away [29].

⁵These one-loop fermion contributions to S and T refer to the standard, rather than holographic, basis, but the two practically coincide, because one-loop corrections from light SM fields are negligible.

⁶The uncalculable contribution to S due to physics at the cut-off scale is $\mathcal{O}(v/\Lambda)^2$. For $\Lambda \sim 10/L$ (see [36]), this is two orders of magnitude smaller than S_{tree} , and thus safely negligible.

⁷We thank A. Strumia for providing us with the updated numerical coefficients entering in the ϵ_i and of the correlation matrix ρ , computed for $M_t = 173.1$ GeV.

where T_{NP} , S_{NP} and $\delta g_{b,NP}$, defined in eq. (A.1), encode the new physics contribution without the SM one and $lh \equiv \log M_{H,eff}/M_Z$, with the effective Higgs mass $M_{H,eff}$ defined as [47]⁸

$$M_{H,eff} = M_H \left(\frac{1}{M_H L} \right)^{\sin^2 \alpha}. \quad (2.18)$$

The experimental values of the ϵ_i , as obtained by LEP1 and SLD data [48, 49], are

$$\begin{aligned} \epsilon_1^{exp} &= (5.03 \pm 0.93) \times 10^{-3}, \\ \epsilon_2^{exp} &= (-7.73 \pm 0.95) \times 10^{-3}, \\ \epsilon_3^{exp} &= (5.44 \pm 0.87) \times 10^{-3}, \\ \epsilon_b^{exp} &= (-6.36 \pm 1.3) \times 10^{-3}. \end{aligned} \quad \rho = \begin{pmatrix} 1 & 0.72 & 0.87 & -0.29 \\ 0.72 & 1 & 0.46 & -0.26 \\ 0.87 & 0.46 & 1 & -0.18 \\ -0.29 & -0.26 & -0.18 & 1 \end{pmatrix}. \quad (2.19)$$

Finally, the χ^2 function is defined as

$$\chi^2 = (\epsilon_i - \epsilon_i^{exp})(\sigma^{-1})_{ij}(\epsilon_j - \epsilon_j^{exp}), \quad \sigma_{ij} = \sigma_i \rho_{ij} \sigma_j. \quad (2.20)$$

The bound on $g_{bt,R}$ in the FBKT₁₀ model is included by adding in quadratures to the χ^2 (2.20) the result coming from $b \rightarrow s\gamma$ decay [28]:

$$g_{bt,R} = (9 \pm 8) \times 10^{-4}. \quad (2.21)$$

Our results have been obtained by performing a random scan on the parameter space of the models. The possibility of having simple analytic approximate formulas for the top and bottom masses considerably helps in the scanning procedure, allowing us to reduce the number of free parameters. In our analysis we take into account in an approximate way the running of the top mass by fixing its value at the energy scale $1/L$ in the range $M_t(1/L) = (150 \pm 5) \text{ GeV}$.

In the next sections we will specify each model separately and present the results of our combined fit.

3 Model I: FBKT₁₀

This is probably the simplest GHU model that can be built, with just one bulk multiplet ξ in the adjoint representation **10** of SO(5). It is also the model with the least number of parameters we consider and probably the one with less parameters so far in the literature. The **10** decomposes as follows under SO(4): **10** = (**2**, **2**) + (**1**, **3**) + (**3**, **1**). The boundary conditions of the LH components of the multiplet ξ are

$$\xi_L = \begin{pmatrix} \left\{ \begin{array}{l} x_L(+ -) \\ u_L(- -) \\ d_L(- -) \end{array} \right. & T_L(+ -) \\ [q'_L(- +), q_L(+ +)] \end{pmatrix}_{\frac{2}{3}}, \quad (3.1)$$

⁸Notice that in eq. (2.18) we have replaced Λ , as taken in [47], with $1/L$, because in GHU models by locality the Higgs contribution to ϵ_i is finite and saturated at the compactification scale $1/L$, rather than at the cut-off of the theory Λ .

where the first and second entries in round brackets refer to the + (−) Neumann (Dirichlet) b.c. at the $y = 0$ (UV) and $y = L$ (IR) branes, respectively. The RH components will have the opposite b.c., as usual. In eq. (3.1), q' and q are two $SU(2)_L$ doublets, with $T_3^R(q') = 1/2$, $T_3^R(q) = -1/2$, which form the $SO(4)$ bidoublet $(\mathbf{2}, \mathbf{2})$, T_L is an $SU(2)_L$ triplet with $T_3^R(T) = 0$ and the states in curly brackets are $SU(2)_L$ singlets forming a triplet of $SU(2)_R$. The subscript 2/3 denotes the $U(1)_X$ charge of the multiplet. We identify the RH components of the top (t_R) and bottom (b_R) fields with the massless modes of the u_R and d_R components respectively.

As explained in section 2, at $y = 0$ we add the most general BKT for the non-vanishing field components there, namely

$$\mathcal{L}_{4f,0} = Z_q \bar{q}_L i \not{D} q_L + Z_t \bar{u}_R i \not{D} u_R + Z_b \bar{d}_R i \not{D} d_R + Z_x \bar{x}_L i \not{D} x_L + Z_T \text{Tr} \bar{T}_L i \not{D} T_L + Z_{q'} \bar{q}'_R i \not{D} q'_R. \quad (3.2)$$

No mass terms are allowed at $y = L$ and hence the IR localized Lagrangian is trivial:

$$\mathcal{L}_{4f,L} = 0. \quad (3.3)$$

The holographic low-energy effective action, with the “bulk” physics integrated out, is up to $\mathcal{O}(s_\alpha^2)$ terms,

$$\mathcal{L}_H = \bar{q}_L \frac{\not{p}}{p} \Pi_0^q q_L + \sum_{a=t,b} \bar{a}_R \frac{\not{p}}{p} \Pi_0^a a_R + \frac{s_\alpha}{h} \left(\Pi_M^t \bar{q}_L H^c t_R + \Pi_M^b \bar{q}_L H b_R + h.c. \right), \quad (3.4)$$

where

$$H = \frac{1}{\sqrt{2}} \begin{pmatrix} h_1 - ih_2 \\ -h_3 - ih_4 \end{pmatrix}, \quad H^c \equiv i\sigma_2 H^\star = -\frac{1}{\sqrt{2}} \begin{pmatrix} h_3 - ih_4 \\ h_1 + ih_2 \end{pmatrix}. \quad (3.5)$$

The explicit expression of the form factors appearing in eq. (3.4) is the following:

$$\Pi_0^q = pZ_q + \Pi_+(c), \quad \Pi_0^{t,b} = pZ_{t,b} - \frac{1}{\Pi_-(m)}, \quad \Pi_M^t = \frac{\Pi_M^b}{\sqrt{2}} = \frac{\Pi_-(m) - \Pi_+(m)}{\sqrt{2}\Pi_-(m)}, \quad (3.6)$$

in terms of the basic form factors

$$\Pi_+(m) = \frac{G_-(m)}{G_+(m)}, \quad \Pi_-(m) = -\frac{G_+(-m)}{G_-(m)}, \quad (3.7)$$

which, in turn, can be expressed in terms of the bulk to boundary fermion propagators

$$G_+(m) = \cos(\omega L) + \frac{m}{\omega} \sin(\omega L), \quad G_-(m) = \frac{p}{\omega} \sin(\omega L), \quad (3.8)$$

with $\omega \equiv \sqrt{p^2 - m^2}$.⁹

Very simple formulas for the top and bottom masses can be obtained by taking the zero momentum limit of the form factors appearing in the Lagrangian (3.4). We have

$$\frac{M_t^2}{M_W^2} \simeq \frac{\theta + 1}{2N_L N_{tR}}, \quad \frac{M_b^2}{M_W^2} \simeq \frac{\theta + 1}{N_L N_{bR}}, \quad (3.9)$$

⁹Notice that the propagators G_\pm in eq. (3.8) differ by a factor ω from those defined in [36]. In the form (3.8), the propagators are real also for imaginary values of ω .

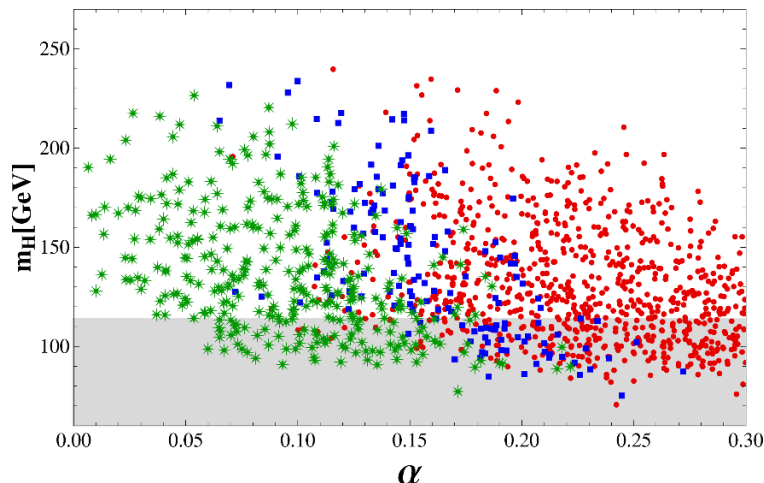


Figure 1. Scatter plot of points obtained from a scan over the parameter space of the FBKT₁₀ model. Small red dots represent points which don't pass EWPT at 99% C.L., square blue dots represent points which pass EWPT at 99% C.L. but not at 90% C.L., and star shape green dots represent points which pass EWPT at 90% C.L.. The region below the LEP bound ($m_H < 114$ GeV) is shaded.

where

$$\begin{aligned}
 N_L &= \lim_{p \rightarrow 0} \frac{\Pi_0^q}{pL} = \frac{Z_q}{L} + \frac{1}{mL(\coth mL + 1)}, \\
 N_{t_R, b_R} &= \lim_{p \rightarrow 0} \frac{\Pi_0^{t,b}}{pL} = \frac{Z_{t,b}}{L} + \frac{1}{mL(\coth mL - 1)}.
 \end{aligned}
 \tag{3.10}$$

Embedding a whole generation in a single bulk multiplet obviously implies that the upper and lower non-canonically normalized Yukawa couplings in the holographic effective Lagrangian (3.4) are necessarily of the same order of magnitude, in our case $|Y_b| = \sqrt{2}|Y_t|$. Thus, the hierarchy between quark masses within a single generation does not arise from field localization in the extra dimension, but by demanding the b_R to be more elementary than t_R , namely by taking the BKT Z_b of b_R much larger than the BKT Z_t of t_R , so that $N_{b_R} \gg N_{t_R}$ and hence $M_b \ll M_t$. The spectrum of fermion resonances beyond the SM, before ElectroWeak Symmetry Breaking (EWSB), is given by KK towers of states in the $\mathbf{2}_{7/6}$, $\mathbf{2}_{1/6}$, $\mathbf{1}_{5/3}$, $\mathbf{1}_{2/3}$, $\mathbf{1}_{-1/3}$ and $\mathbf{3}_{2/3}$ of $SU(2)_L \times U(1)_Y$.

The fermion contribution to the Higgs effective potential is the sum of three terms, coming from the states with $U(1)_Q$ charges $+5/3$, $+2/3$ and $-1/3$. The former contribution, V_{ex} , comes entirely from heavy states, while the latter two, V_t and V_b , are related to the top and bottom KK tower of states. These contributions cannot be written in terms of the form factors appearing in eq. (3.4), since higher order terms in s_α are missing and, moreover, extra contributions arise from the bulk. The latter are absent only in the holographic basis where one chooses as holographic fields all the components of a multiplet with the same chirality [25]. This choice is manifestly not possible if we want to keep the q_L , t_R and b_R components as holographic fields, given that they come from the same bulk field (3.1).

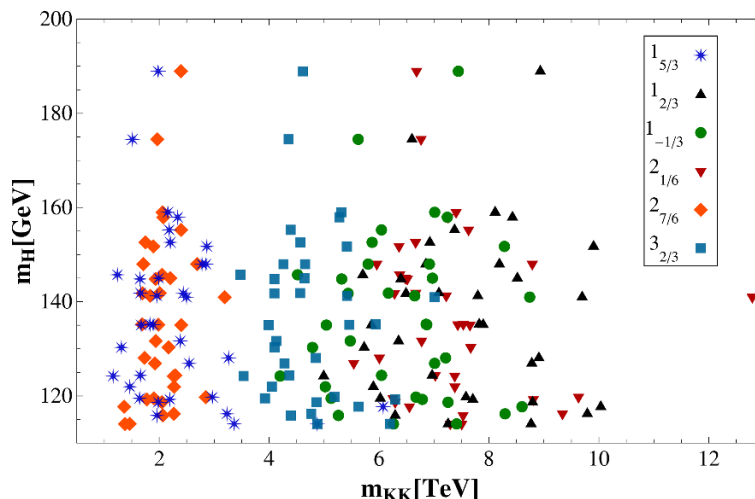


Figure 2. Higgs mass m_H versus the mass of the first KK resonances (before EWSB) for the points of the FBKT₁₀ model with $m_H > 114$ GeV and $\alpha \in [0.16, 0.23]$.

The fermion contributions to the Higgs potential (mainly the top one) is quite lengthy. For simplicity, we report in the following the explicit form of the Higgs potential only in the relevant region in parameter space where $Z_T, Z_q, Z_x \ll 1$ and $Z_b \gg 1$. Neglecting Z_T, Z_q and Z_x , we get

$$\begin{aligned}
 V_t &\simeq -2N_c \int \frac{d^4 p}{(2\pi)^4} \ln \left(1 + s_\alpha^2 \frac{(\Pi_- - \Pi_+) (2p\Pi_+\Pi_- (Z_t - Z_{q'}) + \Pi_- - \Pi_+)}{4\Pi_+\Pi_- (pZ_{q'}\Pi_+ - 1)(pZ_t\Pi_- - 1)} \right), \\
 V_b &\simeq -2N_c \int \frac{d^4 p}{(2\pi)^4} \ln \left(1 + s_\alpha^2 \frac{\Pi_+ - \Pi_-}{2pZ_b\Pi_+\Pi_-} \right), \\
 V_{ex} &\simeq -2N_c \int \frac{d^4 p}{(2\pi)^4} \ln \left(1 + s_\alpha^2 \frac{\Pi_- - \Pi_+}{\Pi_- (pZ_{q'}\Pi_+ - 1)} \right),
 \end{aligned} \tag{3.11}$$

where we have omitted the mass dependence of the form factors Π_\pm . The total Higgs potential is finally

$$V_{\text{tot}} = V_g + V_t + V_b + V_{ex}, \tag{3.12}$$

with V_g given in eq. (2.10).

The tree-level contribution to δg_b at leading order in an expansion in α is

$$\delta g_b = \frac{e^{2mL} m Z_T}{1 - e^{2mL} (1 + 2m Z_q)} \frac{\alpha^2}{2}. \tag{3.13}$$

The deviation (3.13) crucially depends on the BKT of the triplet, Z_T . When the latter vanishes, $\delta g_b = 0$ (this is actually true to all orders in α , at tree-level). This is a consequence of a \mathbf{Z}_2 custodial symmetry [30]. More precisely, $\delta g_b \neq 0$ anytime, after EWSB, b_L sits in 5D fields where $T_3^R \neq T_3^L$ and the deviation is proportional to $(T_3^R - T_3^L)$. In the case at hand, in absence of the BKT, there is a precise cancellation between the contributions of

the $T_3^R = -1, T_3^L = 0$ and of the $T_3^R = 0, T_3^L = -1$ states. This compensation is explicitly broken by Z_T . The mass-dependence of the result has also a simple physical interpretation. Recall that in flat space, depending on the sign of the bulk mass term, KK states with $(+-)$ or $(-+)$ b.c. become light exponentially, with an exponent governed by the mass term m . For $m > 0$, fermions with $(+-)$ b.c. for the LH components become light, while for $m < 0$ fermions with $(-+)$ b.c. for the LH components become light.¹⁰ When $|mL| \gg 1$ and negative, the triplet tower is heavy and δg_b is suppressed, while for positive m the triplet tower becomes ultra-light and δg_b is unsuppressed.

As we mentioned in section 2, in the FBKT₁₀ model the coupling $W t_R b_R$ is generated at tree-level. At the leading order in α , we find

$$g_{bt,R} = -\frac{\alpha^2}{2\sqrt{2}} \frac{e^{2mL} - 1}{2mL\sqrt{N_{tR}N_{bR}}}, \quad (3.14)$$

with N_{tR} and N_{bR} given in eq. (3.10). When $Z_t = Z_b = 0$, $g_{bt,R}$ is unsuppressed and it equals

$$g_{bt,R} = -\frac{\alpha^2}{2\sqrt{2}}, \quad (3.15)$$

which is independent of m . This non-decoupling can heuristically be understood by noticing that when $m < 0$ the masses of the KK states mixing with t_R and b_R are large, but t_R and b_R are more composite (peaked toward the IR brane). On the contrary, when $m > 0$, t_R and b_R are more elementary (UV peaked) but the KK states associated to the q' tower become ultra-light. For any m , the two effects compensate each other, resulting in an unsuppressed $g_{bt,R}$. When Z_b and Z_t are switched on, $g_{bt,R}$ is suppressed by N_{bR} , which is required to be large to correctly reproduce the bottom mass.

3.1 Results

The results of our numerical scan are summarized in figures 1, 2 and 3. The randomly chosen input parameters are $m, Z_q, Z_{q'}, Z_x, Z_T, \theta$ and θ' . The remaining two parameters Z_t and Z_b are fixed by the top and bottom mass formulas. For stability reasons, we take positive coefficients for all the BKT. We have scanned the parameter space over the region $mL \in [-1.5, 0.5]$, $Z_q/L \in [0, 1.5]$, $Z_{q'}/L \in [0, 2]$, $Z_x/L \in [0, 6]$, $Z_T/L \in [0, 1.5]$, $\theta \in [20, 30]$ and $\theta' \in [15, 25]$.

As can be seen in figure 1, the EWPT constrain $\alpha \lesssim 1/5$, with a light Higgs mass for the less-tuned points with $\alpha \simeq 0.15$. The Higgs mass increases only for more tuned configurations with $\alpha < 0.15$. The lightest exotic particles are fermion $SU(2)_L$ singlets with $Y = 5/3$ and $SU(2)_L$ doublets with $Y = 7/6$, see figure 2. After EWSB, these multiplets give rise to $5/3$ and $2/3$ charged fermions. Their mass is of order $1 \div 2$ TeV, significantly lighter than the gauge KK modes (~ 5 TeV). The doublet q_L and the singlet t_R have typically a sizable and comparable degree of compositeness, while b_R is mostly elementary. When $mL \lesssim -1$, q_L turns out to be even more composite than t_R .

¹⁰This is completely analogous to the warped space case, in which, due to a non-vanishing spin connection, the relevant parameters are $m/k \pm 1/2$, where k is the AdS₅ curvature scale.

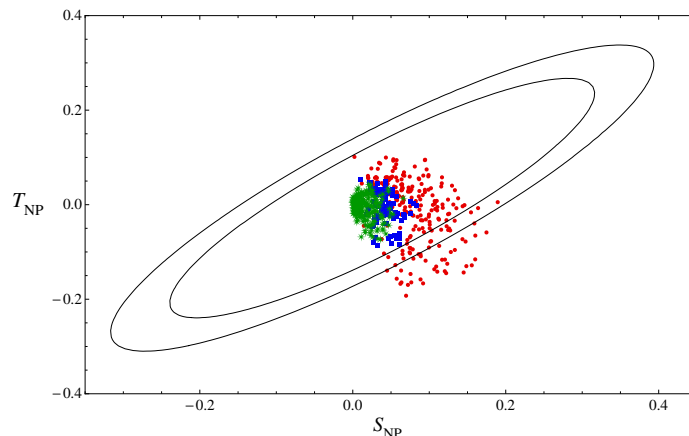


Figure 3. Scatter plot of points in the FBKT₁₀ model with $m_H > 114$ GeV and projected on the T_{NP} - S_{NP} plane. We have set $M_{H,eff} = 120$ GeV. Small red dots represent points which don't pass EWPT at 99% C.L., square blue dots represent points which pass EWPT at 99% C.L. but not at 90% C.L., and star shape green dots represent points which pass EWPT at 90% C.L.. The big and small ellipses correspond to 99% and 90% C.L. respectively.

4 Model II: FBKT₅

The simplest model that can be built by using the fundamental representation of SO(5) is constructed by embedding each generation of SM quarks in two bulk multiplets ξ_t and ξ_b . The **5** decomposes as follows under SO(4): $\mathbf{5} = (\mathbf{2}, \mathbf{2}) \oplus (\mathbf{1}, \mathbf{1})$. The boundary conditions on the fields,

$$\xi_{tL} = \begin{pmatrix} (2, 2)_L^t = \begin{bmatrix} q'_{1L}(-+) \\ q'_{1L}(++) \end{bmatrix} \\ (1, 1)_L^t = u_L(--) \end{pmatrix}_{2/3}, \quad \xi_{bL} = \begin{pmatrix} (2, 2)_L^b = \begin{bmatrix} q_{2L}(++) \\ q'_{2L}(-+) \end{bmatrix} \\ (1, 1)_L^b = d_L(--) \end{pmatrix}_{-1/3}, \quad (4.1)$$

are fixed by the requirement of obtaining, out of each multiplet, the correct set of massless components, namely a left-handed $SU(2)_L$ doublet and one $SU(2)_L$ right-handed singlet. For the third quark generation we can identify the u_R and d_R zero-modes with the top and bottom RH singlets (t_R and b_R). On the other hand, the q_{1L} and q_{2L} zero-modes provide two copies of the LH SM doublet and we need to eliminate a linear combination of the two states from the massless spectrum. This can be easily done by modifying the UV boundary conditions for the doublets and requiring a linear combination of the two left-handed components to satisfy Dirichlet conditions at the $y = 0$ boundary (in our case we choose $(q_{1L} + q_{2L})/\sqrt{2}$ as the SM doublet).¹¹

The most general BKT for the non-vanishing field components at $y = 0$ are

$$\mathcal{L}_{4f,0} = Z_q \bar{q}_L i \not{D} q_L + Z_t \bar{u}_R i \not{D} u_R + Z_b \bar{d}_R i \not{D} d_R + Z_{R1} \bar{q}'_{1R} i \not{D} q'_{1R} + Z_{R2} \bar{q}'_{2R} i \not{D} q'_{2R}. \quad (4.2)$$

¹¹Equivalently one could get rid of the unwanted massless doublet by introducing a right-handed massless fermion doublet localized at the $y = 0$ boundary, which couples to the extra zero-mode with a large mass mixing.

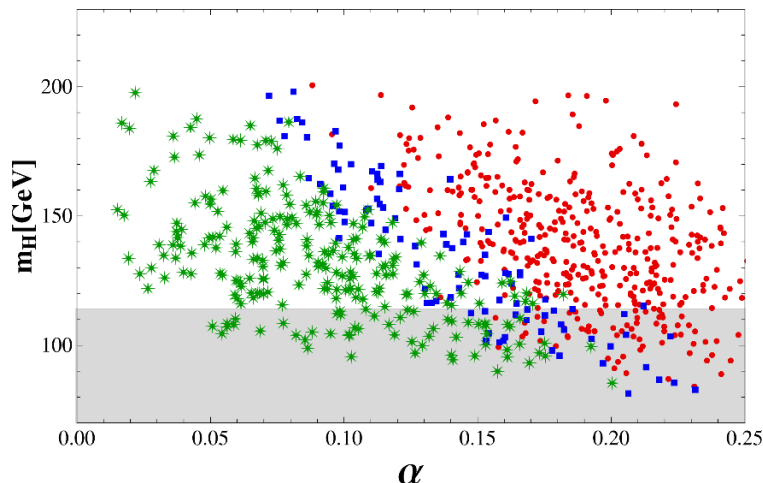


Figure 4. Scatter plot of points obtained from a scan over the parameter space of the FBKT₅ model. Small red dots represent points which don't pass EWPT at 99% C.L., square blue dots represent points which pass EWPT at 99% C.L. but not at 90% C.L., and star shape green dots represent points which pass EWPT at 90% C.L.. The region below the LEP bound ($m_H < 114$ GeV) is shaded.

No mass terms are allowed at $y = L$ and hence the IR localized Lagrangian is trivial:

$$\mathcal{L}_{4f,L} = 0. \tag{4.3}$$

The holographic low-energy effective action is, up to $\mathcal{O}(s_\alpha^2)$ terms, of the form (3.4), where

$$\Pi_0^q = pZ_q + \frac{1}{2}(\Pi_+(m_t) + \Pi_+(m_b)), \tag{4.4}$$

$$\Pi_0^{t,b} = pZ_{t,b} - \frac{1}{\Pi_-(m_{t,b})}, \tag{4.5}$$

$$\Pi_M^{t,b} = \frac{\Pi_-(m_{t,b}) - \Pi_+(m_{t,b})}{\sqrt{2}\Pi_-(m_{t,b})}. \tag{4.6}$$

Simple approximate formulas for the top and bottom masses are obtained from the Lagrangian (3.4). One has

$$\frac{M_t^2}{M_W^2} \simeq \frac{\theta + 1}{2N_L N_{tR}}, \quad \frac{M_b^2}{M_W^2} \simeq \frac{\theta + 1}{2N_L N_{bR}}, \tag{4.7}$$

where

$$N_L = \lim_{p \rightarrow 0} \frac{\Pi_0^q}{pL} = \frac{Z_q}{L} + \frac{1 - e^{-2Lm_t}}{4Lm_t} + \frac{1 - e^{-2Lm_b}}{4Lm_b},$$

$$N_{tR,bR} = \lim_{p \rightarrow 0} \frac{\Pi_0^{t,b}}{pL} = \frac{Z_{t,b}}{L} + \frac{e^{2Lm_{t,b}} - 1}{2Lm_{t,b}}. \tag{4.8}$$

The spectrum of fermion resonances beyond the SM, before EWSB, is given by KK towers of states in the $\mathbf{2}_{7/6}$, $\mathbf{2}_{-5/6}$, $\mathbf{2}_{1/6}$, $\mathbf{1}_{2/3}$ and $\mathbf{1}_{-1/3}$ of $SU(2)_L \times U(1)_Y$.

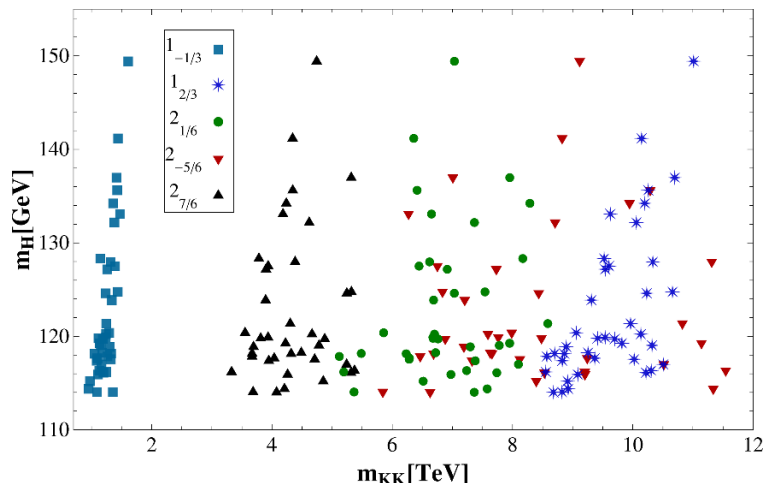


Figure 5. Higgs mass m_H versus the mass of the first KK resonances (before EWSB) for the points of the FBKT₅ model with $m_H > 114$ GeV and $\alpha \in [0.16, 0.22]$.

The fermion contribution to the Higgs effective potential cannot be written in terms of the form factors appearing in eq. (3.4) for the same reasons explained for the FBKT₁₀ model above eq. (3.11). The fermion contribution to the Higgs potential comes from the top and bottom tower of states, $V_f = V_t + V_b$. The explicit form of the top tower contribution to the potential is given by

$$V_t = -2N_c \int \frac{d^4 p}{(2\pi)^4} \ln \left[1 + \sin^2 \alpha \frac{\Pi_+(m_t) - \Pi_-(m_t)}{2(pZ_t \Pi_-(m_t) - 1)} \left(pZ_t + p \frac{Z_{R1} - Z_t}{pZ_{R1} \Pi_+(m_t) - 1} - \frac{pZ_t \Pi_+(m_t) - 1}{2pZ_q + \Pi_+(m_t) + \Pi_+(m_b)} \right) \right], \quad (4.9)$$

while the bottom tower contribution V_b is obtained from V_t by the replacements $t \leftrightarrow b$ and $Z_{R1} \rightarrow Z_{R2}$. The total Higgs potential is finally

$$V_{\text{tot}} = V_g + V_t + V_b, \quad (4.10)$$

with V_g given in eq. (2.10).

The tree-level contribution to δg_b at leading order in an expansion in α is

$$\delta g_b = \frac{1 - e^{-2m_b L}}{16m_b L N_L} \alpha^2. \quad (4.11)$$

The result (4.11) has a simple physical interpretation. According to the analysis of [30], multiplets in which the bottom lives only in components with $T_3^R = T_3^L$ do not contribute to δg_b . This condition is satisfied by the ξ_t multiplet, hence the only corrections come from the ξ_b field. A comparison with eq. (4.8) shows that, as expected, the correction to g_{bL} is an $\mathcal{O}(\alpha^2)$ effect and is proportional to the fraction of the b_L wave function which lives in the ξ_b multiplet, which is encoded in the ratio on the right hand side of eq. (4.11).

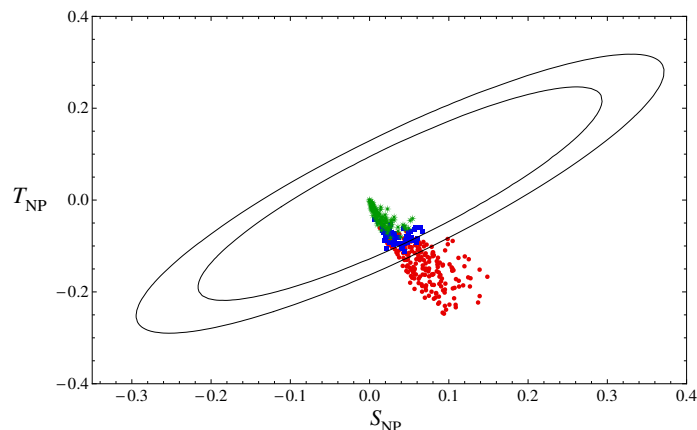


Figure 6. Scatter plot of points in the FBKT₅ model with $m_H > 114$ GeV and projected on the T_{NP} - S_{NP} plane. We have set $M_{H,eff} = 120$ GeV. Small red dots represent points which don't pass EWPT at 99% C.L., square blue dots represent points which pass EWPT at 99% C.L. but not at 90% C.L., and star shape green dots represent points which pass EWPT at 90% C.L.. The big and small ellipses correspond to 99% and 90% C.L. respectively.

4.1 Results

The results of our numerical scan are summarized in figures 4, 5 and 6. The randomly chosen input parameters are m_t , m_b , Z_{R1} , Z_{R2} , Z_q , θ and θ' . The remaining two parameters Z_b and Z_t are fixed by the top and bottom mass formulas. For stability reasons, we take positive coefficients for all the BKT and $m_b L \gtrsim 1$ in order to suppress δg_b , as given by eq. (4.11). More precisely, we have taken $m_t L \in [0.1, 1.3]$, $m_b L \in [2, 2.5]$, $Z_{R1}/L \in [0.1, 1.6]$, $Z_{R2}/L \in [0, 1]$, $Z_q/L \in [0.5, 2]$, $\theta \in [15, 25]$, $\theta' \in [15, 25]$. As can be seen in figure 4, the EWPT constrain $\alpha \simeq 1/5$, with a very light Higgs mass. The latter increases only for more tuned configurations with $\alpha < 0.15$. Interestingly enough, the lightest exotic particle is always a fermion singlet with $Q = -1/3$, see figure 5. Its mass is of order 1 TeV, significantly lighter than the gauge KK modes (~ 5 TeV) and the other fermion resonances, with masses starting from around 4 TeV. The doublet q_L is generically semi-composite, the singlet t_R is mostly composite and b_R is mostly elementary.

5 Model III: modified MCHM₅

The last model we consider is the flat space version of one of the models considered in [33] and denoted there MCHM₅. It was already noticed in [36] that this model can lead to realistic theories also when defined on a flat segment, provided large BKT for the gauge fields are included. Here we perform a systematic analysis of the electroweak bounds in this model, that was neither made in [36] nor in [33]. We describe very briefly the model, referring the reader to section 4.2 of [36] or to the original warped space version [33] for further details. Fermion BKT can also be introduced in this model, of course, but given the larger number of parameters present in this model with respect to the FBKT models, we have decided, for simplicity, to neglect them.

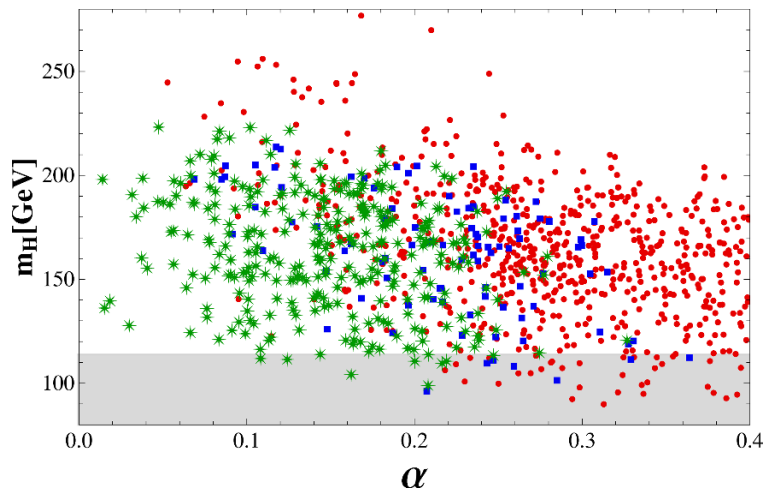


Figure 7. Scatter plot of points obtained from a scan over the parameter space of MCHM₅. Small red dots represent points which don't pass EWPT at 99% C.L., square blue dots represent points which pass EWPT at 99% C.L. but not at 90% C.L., and star shape green dots represent points which pass EWPT at 90% C.L.. The region below the LEP bound ($m_H < 114$ GeV) is shaded.

The SM quarks are embedded in bulk fermions transforming in the fundamental representation of SO(5). For each quark generation, 4 bulk fermions $\xi_{q_1}, \xi_{q_2}, \xi_u$ and ξ_d in the **5** are introduced. The holographic Lagrangian for the third quark generation can be written to all orders in s_α and has the simple form

$$\begin{aligned} \mathcal{L}_H = & \bar{q}_L \frac{\not{p}}{p} \left[\Pi_0^q + s_\alpha^2 \left(\Pi_1^{qu} \frac{H^c(H^c)^\dagger}{H^\dagger H} + \Pi_1^{qd} \frac{H H^\dagger}{H^\dagger H} \right) \right] q_L + \sum_{a=u,d} \bar{a}_R \frac{\not{p}}{p} \left(\Pi_0^a + s_\alpha^2 \Pi_1^a \right) a_R \\ & + \frac{s_2 \alpha}{2h} \left(\Pi_M^u \bar{q}_L H^c u_R + \Pi_M^d \bar{q}_L H d_R + h.c. \right). \end{aligned} \tag{5.1}$$

The expression of the form factors appearing in eq. (5.1) is reported in eq. (C.3) of [36]. The top and bottom quark masses are approximately given by

$$\frac{M_t^2}{M_W^2} \simeq \frac{\theta |\tilde{m}_u - \tilde{M}_u^{-1}|^2 e^{2L(m_u - m_1)}}{N_L N_{uR}}, \quad \frac{M_b^2}{M_W^2} \simeq \frac{\theta |\tilde{m}_d - \tilde{M}_d^{-1}|^2 e^{2L(m_d - m_2)}}{N_L N_{dR}}, \tag{5.2}$$

where

$$\begin{aligned} N_L &= \lim_{p \rightarrow 0} \frac{\Pi_0^q}{pL} = \frac{1}{L} \sum_{i=u,d,q_1,q_2} \int_0^L dy f_{iL}^2(y), \\ N_{uR} &= \lim_{p \rightarrow 0} \frac{\Pi_0^u}{pL} = \frac{1}{L} \int_0^L dy \left(f_{uR}^2(y) + f_{q_1R}^2(y) \right), \\ N_{dR} &= \lim_{p \rightarrow 0} \frac{\Pi_0^d}{pL} = \frac{1}{L} \int_0^L dy \left(f_{dR}^2(y) + f_{q_2R}^2(y) \right), \end{aligned} \tag{5.3}$$

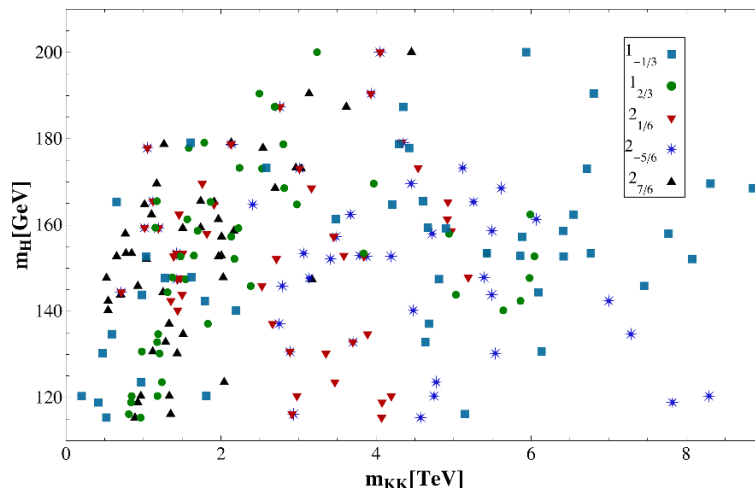


Figure 8. Higgs mass m_H versus the mass of the first KK resonances (before EWSB) for the points of the MCHM₅ model with $m_H > 114$ GeV and $\alpha \in [0.26, 0.34]$.

with $f_{iL,iR}(y)$ the “holographic” wave functions of the LH/RH top and bottom quarks before EWSB. They read

$$\begin{aligned}
 f_{q_1L} &= e^{-m_1 y}, & f_{q_2L} &= e^{-m_2 y}, & f_{uL} &= -\tilde{m}_u e^{-m_1 L + m_u(L-y)}, & f_{dL} &= -\tilde{m}_d e^{-m_2 L + m_d(L-y)}, \\
 f_{uR} &= e^{m_u y}, & f_{q_1R} &= \frac{1}{\tilde{M}_u} e^{m_u L - m_1(L-y)}, & f_{dR} &= e^{m_d y}, & f_{q_2R} &= \frac{1}{\tilde{M}_d} e^{m_d L - m_2(L-y)}.
 \end{aligned}
 \tag{5.4}$$

The spectrum of fermion resonances beyond the SM, before EWSB, is given by KK towers of states in the $\mathbf{2}_{7/6}$, $\mathbf{2}_{-5/6}$, $\mathbf{2}_{1/6}$, $\mathbf{1}_{2/3}$ and $\mathbf{1}_{-1/3}$ of $SU(2)_L \times U(1)_Y$. The fermion contribution to the one-loop Higgs effective potential in this model arises only from the KK towers of the charge $+2/3$ and $-1/3$ states, and can easily be expressed in terms of the form factors appearing in eq. (5.1). We have $V_f = V_t + V_b$, with

$$V_i = -2N_c \int \frac{d^4 p}{(2\pi)^4} \log \left[\left(1 + s_\alpha^2 \frac{\Pi_1^{q_i}}{\Pi_0^q} \right) \left(1 + s_\alpha^2 \frac{\Pi_1^i}{\Pi_0^i} \right) - s_{2\alpha}^2 \frac{(\Pi_M^i)^2}{8\Pi_0^q \Pi_0^i} \right], \quad i = t, b.
 \tag{5.5}$$

The total Higgs potential is

$$V_{\text{tot}} = V_g + V_t + V_b,
 \tag{5.6}$$

with V_g given in eq. (2.10).

The tree-level contribution to δg_b at leading order in an expansion in α is

$$\delta g_b = \frac{\alpha^2}{2N_L} \sum_{i=u,d,q_1,q_2} (T_{3,i}^R - T_3^L) \int_0^L dy \left[\frac{y}{L} (f_{iL}^2 + f_{iL} \delta f_{iL}) + \frac{1}{2} \delta f_{iL}^2 \right],
 \tag{5.7}$$

where $T_3^L = -1/2$, $T_{3,i}^R$ is the $SU(2)_R$ isospin of the corresponding bidoublet component where the b_L lives, f_{iL} are the holographic wave functions of the bidoublet components of the 5D multiplets, reported in the first line of eq. (5.4), and $\delta f_{iL} = f_{iL} - f_{iL}^s$, with f_{iL}^s the

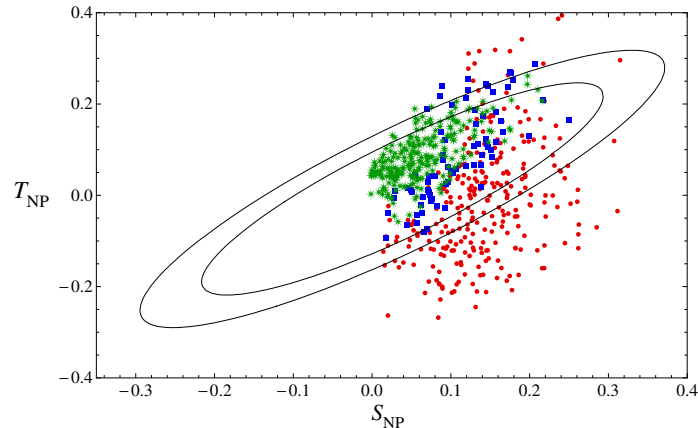


Figure 9. Scatter plot of points in the MCHM₅ model with $m_H > 114$ GeV and projected on the T_{NP} - S_{NP} plane. We have set $M_{H,eff} = 120$ GeV. Star shape red dots represent points which don't pass EWPT at 99% C.L., small blue dots represent points which pass EWPT at 99% C.L. but not at 90% C.L., and big green dots represent points which pass EWPT at 90% C.L.. The big and small ellipses correspond to 99% and 90% C.L. respectively.

holographic wave functions of the singlet components of the 5D multiplets. Only multiplets where $T_3^R \neq T_3^L$ contribute to δg_b , as expected [30]. We have $T_{3,q_1}^R = T_{3,u}^R = -1/2$, $T_{3,q_2}^R = T_{3,d}^R = 1/2$, so that only the latter contribute to δg_b . We also have $f_{q_2L}^s = f_{q_2L}$ and $f_{dL}^s = \tilde{M}_d/\tilde{m}_d f_{dL}$.

5.1 Results

The results of our numerical scan are summarized in figures 7, 8 and 9. The randomly chosen input parameters are m_u , m_d , m_1 , m_2 , \tilde{m}_u , \tilde{m}_d , θ and θ' . The remaining two parameters \tilde{M}_u and \tilde{M}_d are fixed by the top and bottom mass formulas. Demanding a small δg_b at tree-level requires $m_2L \gtrsim 1$, as can be verified by using eq. (5.7). We have scanned the parameter space over the region $m_uL \in [-3, 3]$, $m_dL \in [-5, 2.5]$, $m_1L \in [-2, 2]$, $m_2L \in [2.2, 4.5]$, $\tilde{m}_u \in [-2.3, 4.1]$, $\tilde{m}_d \in [-3.5, 4]$, $\theta \in [17, 27]$, $\theta' \in [14, 26]$. As can be seen in figure 7, the EWPT constraints are now milder, with $\alpha \simeq 1/3$. The Higgs is still light, but now masses up to 200 GeV can be reached in the less-tuned region $\alpha \simeq 1/3$. There is no definite pattern for the lightest exotic particles. As far as collider physics is concerned, this model is the most interesting one, having a scale of new physics lower than that associated to the FBKT models and fermion states below the TeV scale. As expected, b_R is always mostly elementary, while q_L and t_R typically show a sizable degree of compositeness. Depending on the region in parameter space, q_L can be semi-composite and t_R mostly composite or the other way around, with q_L mostly composite and t_R semi-composite.

6 Comments on the EWPT

We give in this section a rough qualitative picture of how the EWPT are passed in each model. We do not try to perform here an analysis of how EWSB selects the fermion mass spectra reported in figures 2, 5 and 8, but rather we take these spectra for granted. An obvious feature common to all the models is $S_{NP} > 0$, coming from the dominant tree-level contribution (2.7). As well-known, given $S_{NP} > 0$, the EWPT favours a light Higgs and models where $T_{NP} > 0$ rather than $T_{NP} < 0$. As far as δg_b is concerned, by comparing eq. (2.17) with eq. (2.19), one finds that models where $\delta g_{b,NP} < 0$ are slightly favoured with respect to the ones with $\delta g_{b,NP} > 0$. Let us now turn to each model separately.

In the FBKT₁₀ model, the lightest resonances before EWSB are the first KK states of the exotic $\mathbf{1}_{5/3}$ and $\mathbf{2}_{7/6}$ towers, see figure 2. The charge 5/3 states do not contribute to $\delta g_{b,NP}$ at one-loop level, and their contribution to T_{NP} is negligible with respect to the one given by the charge 2/3 states (compare eq. (A.14) with eq. (A.24)). The latter contribution to T_{NP} is always negative. The FBKT₁₀ model features an $SU(2)_L$ triplet state, whose tree-level contribution to $\delta g_{b,NP}$ can be sizable and can play an important role in the EWPT. The total combination of these effects does not allow to have large enough values of α , which is then constrained to be at most $\alpha \sim 0.2$.

In the FBKT₅ model, the lightest resonances before EWSB are the first KK states of the $\mathbf{1}_{-1/3}$ tower. As we already remarked, such states have a small overlap with the bottom quark and hence a negligible contribution to S_{NP} , T_{NP} and $\delta g_{b,NP}$. The next to lightest resonances are the two towers of states in the $\mathbf{2}_{1/6}$ and $\mathbf{2}_{7/6}$, which have comparable Yukawa couplings with the top quark. By $SO(4)$ symmetry, the net contributions to T_{NP} and $\delta g_{b,NP}$ of these two states tend to compensate each other. Since typically the $\mathbf{2}_{7/6}$ states are lighter than the $\mathbf{2}_{1/6}$ ones, we get a net negative contribution to T_{NP} and a negligible contribution to $\delta g_{b,NP}$, since the doublets contribution to $\delta g_{b,NP}$ is suppressed (see eqs. (A.11) and (A.16)). In this situation, δg_b is sub-dominant and we get the quite standard behaviour depicted in figure 6, with $S_{NP} > 0$ and $T_{NP} < 0$.

The MCHM₅ model is the most interesting and complicated to analyze, given also the more intricate pattern of fermion spectrum depicted in figure 8. The tree-level contribution to δg_b is typically positive but small. The novelty of this model with respect to the FBKT ones is the appearance of configurations satisfying EWPT with a sizable positive T_{NP} , see figure 9. This is related to two features appearing in the MCHM₅ model. The first is the possibility of having a moderate hierarchy between the Yukawa couplings λ_1 and λ_7 of the lightest states $\mathbf{2}_{1/6}$ and $\mathbf{2}_{7/6}$ with the top quark. It arises thanks to the presence of four bulk fields and IR mass terms, that lead to a larger $SO(5)$ symmetry breaking with respect to the FBKT models. As in the FBKT₅ model, the $\mathbf{2}_{7/6}$ states are lighter than the $\mathbf{2}_{1/6}$ ones (with the singlet $\mathbf{1}_{1/3}$ considerably heavier than both), but it often happens that $\lambda_1 > \lambda_7$ resulting in a net dominance of the $\mathbf{2}_{1/6}$ state with respect to the $\mathbf{2}_{7/6}$ (a similar pattern arises in a specific region in parameter space of the warped model studied in [35]). The total result is a sizable $T_{NP} > 0$ and a negligibly small $\delta g_{b,NP}$. The second feature is the possibility of having light singlet $\mathbf{1}_{2/3}$ states (compare figures 2 and 5 with figure 8). In the FBKT models, the $\mathbf{1}_{2/3}$ states always have $(++)$ or $(--)$ b.c. and are hence heavy,

while in the MCHM₅ model, due to the presence of more bulk fields and IR mass terms, they have mixed b.c. and can be light. Their presence is important, because they positively contribute to T_{NP} . Taken alone, the singlets would also give rise to unacceptably positive and large contributions to $\delta g_{b,NP}$, but it turns out that the net effect of the $\mathbf{2}_{1/6}$, $\mathbf{2}_{7/6}$ and $\mathbf{1}_{2/3}$ states is to keep $\delta g_{b,NP}$ small, while having T_{NP} positive and sizable. We do not exclude that other patterns may exist, where the same desired configuration of $T_{NP} > 0$ and $\delta g_{b,NP} \simeq 0$ is obtained.

7 Conclusions

We have constructed three different composite Higgs/GHU models in flat space with large BKT, based on the minimal custodially-symmetric $\text{SO}(5) \times \text{U}(1)_X$ gauge group, and we have shown that EWSB and EWPT are compatible in these models. We stress that model building in this context is significantly simpler than in warped space.

The Higgs is predicted to be light with a mass $m_H \leq 200 \text{ GeV}$. The lightest new-physics particles are colored fermions with a mass as low as about 500 GeV in the MCHM₅ model and 1 TeV in the FBKT models. Their electroweak quantum numbers depend on the model and on the region in parameter space, but they are always particles with electric charges $-1/3$, $+2/3$ or $+5/3$.

The next step in constructing fully realistic models would be the addition of the light two quark generations, leptons, and flavour in general. We expect that the typical known patterns of flavour physics in warped space, such as the so-called RS-GIM, should also be captured by our effective flat space description. Indeed, in presence of large BKT, the cut-off of the theory becomes effectively a function of the position in the internal space and is maximal at the UV brane, with the SM fields becoming more elementary (peaked at the UV brane at $y = 0$) and the KK states more composite (peaked at the IR brane at $y = L$). In this way, otherwise too large flavour-changing violating operators might be naturally suppressed. It would be very interesting to study this issue in detail and see whether and to what extent this expectation is valid.

The very broad collider signatures of our models completely fall into those of composite Higgs/warped GHU models. The correct EWSB pattern in all composite Higgs/GHU models constructed so far (warped or flat, with $\text{SO}(5)$ or $\text{SU}(3)$ gauge groups) seems to indicate that the lightest (below TeV) new physics states beyond the SM should be fermionic colored particles, with model-dependent $\text{SU}(2)_L \times \text{U}(1)_Y$ quantum numbers. Of course, this generic prediction cannot be seen as a “signature” of composite Higgs/GHU models. More specific predictions are the expected sizable deviations to the SM Higgs-gauge couplings or to the SM top couplings, but at this stage of the LHC run these are details that cannot be detected in the short term.

Acknowledgments

G.P. would like to thank Andrea Wulzer for useful discussions and comments. M.S. thanks Eduardo Pontón and José Santiago for a useful correspondence and especially Alessandro

Strumia for having provided us with the updated numerical coefficients entering in our fit.

A One-loop fermion contribution to the S , T parameters and the $Zb_L\bar{b}_L$ vertex

We collect in this appendix the one-loop fermion contribution to T , S and δg_b in particular limits where relatively simple analytic expressions are available. This is motivated by the fact that often in our models one or two fermion states are significantly lighter than the others and dominate the loop corrections. The SM quantum numbers of these light fermion states vary along the parameter space and thus it can be useful to list the single fermion contribution to T , S and δg_b . We compute the one-loop contribution to δg_b in the approximation in which the external momentum of the Z is set to zero (see [50] for a more general computation). The contribution of the first two light quark generations, including their KK towers, given their light masses and small Yukawa couplings with the KK modes, is expected to be negligible. We have actually checked that even the fermion mixing in the bottom sector is negligible, so that only the charge $+2/3$ states mixing with the top quark should be considered. We define in what follows by T_{NP} , S_{NP} and $\delta g_{b,NP}$ the fermion one-loop contribution given by new physics only, with the SM contribution subtracted:

$$T_{NP} = T - T_{SM}, \quad S_{NP} = S - S_{SM}, \quad \delta g_{b,NP} = \delta g_b - \delta g_{b,SM}, \quad (\text{A.1})$$

where

$$\begin{aligned} g_{b,SM} &= -\frac{1}{2} + \frac{1}{3}s_W^2, & T_{SM} &\simeq \frac{N_c r}{16\pi s_W^2}, & S_{SM} &= \frac{N_c}{18\pi} \left(3 + \log \left(\frac{M_b^2}{M_t^2} \right) \right), \\ \delta g_{b,SM} &= \frac{\alpha_{em}}{16\pi s_W^2} \frac{r(r^2 - 7r + 6 + (2 + 3r) \log r)}{(r - 1)^2}, & r &\equiv \frac{M_t^2}{M_W^2}, \end{aligned} \quad (\text{A.2})$$

$s_W \equiv \sin \theta_W$, and M_t is the pole top mass, $M_t = 173.1$ GeV [51].

We do not exploit the full SO(5) symmetry underlying our model and classify the new fermion states by their SM quantum numbers. In this way, the explicit SO(5) symmetry breaking effects due to the UV b.c., that can be sizable, are taken into account and more reliable expressions are obtained. For simplicity, we take in the following all Yukawa couplings to be real, the extension to complex ones being straightforward.

A.1 Singlet with $Y = 2/3$

The simplest situation arises when the top quark mixes with just one SM singlet vector-like fermion X with hypercharge $Y = 2/3$. The two possible Yukawa couplings are

$$\mathcal{L} \supset y_t \bar{q}_L H^c t_R + y_X \bar{q}_L H^c X_R + h.c. \rightarrow \lambda_t \bar{t}_L t_R + \lambda_X \bar{t}_L X_R + h.c., \quad (\text{A.3})$$

where here and in the following we use the notation that $\lambda_i = y_i v / \sqrt{2}$ is the mass parameter corresponding to the Yukawa coupling y_i . The λ_i are assumed to be small with respect

to the vector-like mass M_X of the new exotic fermions. By using standard techniques and keeping the leading order terms in the λ_i/M_X expansion, we get

$$T_{NP} = \frac{N_c \lambda_X^2 \left(2\lambda_t^2 \log\left(\frac{M_X^2}{\lambda_t^2}\right) + \lambda_X^2 - 2\lambda_t^2 \right)}{16\pi s_W^2 M_W^2 M_X^2}, \quad (\text{A.4})$$

$$S_{NP} = \frac{N_c \lambda_X^2 \left(2\log\left(\frac{M_X^2}{\lambda_t^2}\right) - 5 \right)}{18\pi M_X^2}, \quad (\text{A.5})$$

$$\delta g_{b,NP} = \frac{\alpha_{em} \lambda_X^2 \left(2\lambda_t^2 \log\left(\frac{M_X^2}{\lambda_t^2}\right) + \lambda_X^2 - 2\lambda_t^2 \right)}{16\pi s_W^2 M_W^2 M_X^2}, \quad (\text{A.6})$$

in agreement with [31, 32, 47]. For simplicity, in eq. (A.6) we have only reported the leading order terms in the limit $\lambda_i/M_W \gg 1$. The top mass is given by

$$M_t \simeq \lambda_t \left(1 - \frac{\lambda_X^2}{2M_X^2} \right). \quad (\text{A.7})$$

As can be seen from eqs. (A.4)–(A.6), for a sufficiently large M_X , T_{NP} and $\delta g_{b,NP}$ are closely related and positive (like S_{NP}).

A.2 Doublet with $Y = 1/6$

The two possible Yukawa couplings mixing the top with a new doublet Q_1 with hypercharge $Y = 1/6$ are

$$\mathcal{L} \supset y_i \bar{q}_L H^c t_R + y_1 \bar{Q}_{1L} H^c t_R + h.c. \rightarrow \lambda_t \bar{t}_L t_R + \lambda_1 \bar{Q}_{1uL} t_R + h.c.. \quad (\text{A.8})$$

We find

$$T_{NP} = \frac{N_c \lambda_1^2 \left(6\lambda_t^2 \log\left(\frac{M_1^2}{\lambda_t^2}\right) + 2\lambda_1^2 - 9\lambda_t^2 \right)}{24\pi s_W^2 M_W^2 M_1^2}, \quad (\text{A.9})$$

$$S_{NP} = \frac{N_c \lambda_1^2 \left(4\log\left(\frac{M_1^2}{\lambda_t^2}\right) - 7 \right)}{18\pi M_1^2}, \quad (\text{A.10})$$

$$\delta g_{b,NP} = \frac{\alpha_{em} \lambda_1^2 \lambda_t^2 \log\left(\frac{M_1^2}{\lambda_t^2}\right)}{32\pi s_W^2 M_W^2 M_1^2}, \quad (\text{A.11})$$

in agreement with [31, 32]. The top mass is given by

$$M_t \simeq \lambda_t \left(1 - \frac{\lambda_1^2}{2M_1^2} \right). \quad (\text{A.12})$$

As can be seen from eqs. (A.9)–(A.11), for a sufficiently large M_1 , T_{NP} , $\delta g_{b,NP}$ and S_{NP} are all positive.

A.3 Doublet with $Y = 7/6$

The two possible Yukawa couplings mixing the top with a new doublet Q_7 with hypercharge $Y = 7/6$ are

$$\mathcal{L} \supset y_t \bar{q}_L H^c t_R + y_7 \bar{Q}_{7L} H t_R + h.c. \rightarrow \lambda_t \bar{t}_L t_R + \lambda_7 \bar{Q}_{7dL} t_R + h.c.. \quad (\text{A.13})$$

We find

$$T_{NP} = -\frac{N_c \lambda_7^2 \left(6\lambda_t^2 \log\left(\frac{M_7^2}{\lambda_t^2}\right) - 2\lambda_7^2 - 9\lambda_t^2 \right)}{24\pi s_W^2 M_W^2 M_7^2}, \quad (\text{A.14})$$

$$S_{NP} = -\frac{N_c \lambda_7^2 \left(4 \log\left(\frac{M_7^2}{\lambda_t^2}\right) - 15 \right)}{18\pi M_7^2}, \quad (\text{A.15})$$

$$\delta g_{b,NP} = -\frac{\alpha_{em} \lambda_7^2 \lambda_t^2 \log\left(\frac{M_7^2}{\lambda_t^2}\right)}{32\pi s_W^2 M_W^2 M_7^2}, \quad (\text{A.16})$$

in agreement with [31, 32]. The top mass is given by

$$M_t \simeq \lambda_t \left(1 - \frac{\lambda_7^2}{2M_7^2} \right). \quad (\text{A.17})$$

As can be seen from eqs. (A.14)–(A.16), for a sufficiently large M_7 , T_{NP} , $\delta g_{b,NP}$ and S_{NP} are all negative.

The contributions to T , S and δg_b of the doublets with $Y = 1/6$ and $Y = 7/6$ are almost the same in magnitude, but opposite in sign. When present together, then, there tends to be a partial cancellation among these two contributions. In the SO(4) invariant limit in which $M_1 = M_7$ and $\lambda_1 = \lambda_7$, their contributions to T and δg_b precisely cancel.

A.4 Triplet with $Y = 2/3$

The two possible Yukawa couplings mixing the top with a new triplet T with hypercharge $Y = 2/3$ are

$$\mathcal{L} \supset y_t \bar{q}_L H^c t_R + \sqrt{2} y_T \bar{q}_L T_R H^c + h.c. \rightarrow \lambda_t \bar{t}_L t_R + \lambda_T \bar{t}_L T_{0R} + h.c., \quad (\text{A.18})$$

where $T_{0,R}$ is the triplet component with $T_{3L} = 0$. We find

$$T_{NP} = \frac{N_c \lambda_T^2 \left(18\lambda_t^2 \log\left(\frac{M_T^2}{\lambda_t^2}\right) + 19\lambda_T^2 - 30\lambda_t^2 \right)}{48\pi s_W^2 M_W^2 M_T^2}, \quad (\text{A.19})$$

$$S_{NP} = -\frac{N_c \lambda_T^2 \left(4 \log\left(\frac{M_T^3 \lambda_t}{\lambda_b^4}\right) - 29 \right)}{18\pi M_T^2}, \quad (\text{A.20})$$

$$\delta g_{b,NP} = -\frac{\alpha_{em} \lambda_T^2 \left(2\lambda_t^2 \log\left(\frac{M_T^2}{\lambda_t^2}\right) - \lambda_T^2 \right)}{16\pi s_W^2 M_W^2 M_T^2}. \quad (\text{A.21})$$

The top mass is given by

$$M_t \simeq \lambda_t \left(1 - \frac{\lambda_T^2}{2M_T^2} \right). \quad (\text{A.22})$$

As can be seen from eqs. (A.19)–(A.21), $T_{NP} > 0$ and $\delta g_{b,NP} < 0$. Contrary to the previous cases, the bottom quark mixing cannot consistently be neglected, since the same Yukawa coupling in eq. (A.18) mixing the top with the $T_{3L} = 0$ triplet component gives also a mixing between the bottom and the $T_{3L} = -1$ triplet component. This mixing is at the origin of the log term involving the bottom Yukawa coupling λ_b in eq. (A.20), which enhances the fermion one-loop contribution to S with respect to the previous cases and gives $S_{NP} < 0$.

A.5 Doublet with $Y = 7/6$ mixing with singlet with $Y = 5/3$

The two Yukawa couplings mixing a vector-like singlet X with hypercharge $Y = 5/3$ with a vector-like doublet Q_7 with $Y = 7/6$ are

$$\mathcal{L} \supset y_{XL} \bar{Q}_{7R} H^c X_L + y_{XR} \bar{Q}_{7L} H^c X_R + h.c. \rightarrow \lambda_{XL} \bar{Q}_{7uR} X_L + \lambda_{XR} \bar{Q}_{7uL} X_R + h.c.. \quad (\text{A.23})$$

In the limit in which $M_7 = M_X$, we have

$$T_{NP} = \frac{N_c \left(13\lambda_{XL}^4 + 2\lambda_{XL}^3 \lambda_{XR} + 18\lambda_{XL}^2 \lambda_{XR}^2 + 2\lambda_{XL} \lambda_{XR}^3 + 13\lambda_{XR}^4 \right)}{480\pi s_W^2 M_W^2 M_X^2}, \quad (\text{A.24})$$

$$S_{NP} = \frac{N_c \left(12\lambda_{XL}^2 + 79\lambda_{XL} \lambda_{XR} + 12\lambda_{XR}^2 \right)}{90\pi M_X^2}. \quad (\text{A.25})$$

Of course, δg_b vanishes, since there is no coupling between the bottom and these states. Being given by vector-like states, eqs. (A.24) and (A.25) do not contain “large” log’s of the form $\log M/\lambda_t$. Assuming equality of masses and Yukawa’s, the contribution to T in eq. (A.24) is suppressed with respect to the other contributions previously determined.

References

- [1] D.B. Fairlie, *Higgs’ Fields and the Determination of the Weinberg Angle*, *Phys. Lett.* **B 82** (1979) 97 [SPIRES].
- [2] D.B. Fairlie, *Two Consistent Calculations Of The Weinberg Angle*, *J. Phys.* **G 5** (1979) L55.
- [3] N.S. Manton, *A New Six-Dimensional Approach to the Weinberg-Salam Model*, *Nucl. Phys.* **B 158** (1979) 141 [SPIRES].
- [4] P. Forgacs and N.S. Manton, *Space-Time Symmetries in Gauge Theories*, *Commun. Math. Phys.* **72** (1980) 15 [SPIRES].
- [5] Y. Hosotani, *Dynamical Mass Generation by Compact Extra Dimensions*, *Phys. Lett.* **B 126** (1983) 309 [SPIRES].
- [6] Y. Hosotani, *Dynamical Gauge Symmetry Breaking as the Casimir Effect*, *Phys. Lett.* **B 129** (1983) 193 [SPIRES].
- [7] Y. Hosotani, *Dynamics of Nonintegrable Phases and Gauge Symmetry Breaking*, *Ann. Phys.* **190** (1989) 233 [SPIRES].
- [8] L. Randall and R. Sundrum, *A large mass hierarchy from a small extra dimension*, *Phys. Rev. Lett.* **83** (1999) 3370 [hep-ph/9905221] [SPIRES].

- [9] L. Randall and R. Sundrum, *An alternative to compactification*, *Phys. Rev. Lett.* **83** (1999) 4690 [[hep-th/9906064](#)] [[SPIRES](#)].
- [10] N. Arkani-Hamed, M. Porrati and L. Randall, *Holography and phenomenology*, *JHEP* **08** (2001) 017 [[hep-th/0012148](#)] [[SPIRES](#)].
- [11] R. Rattazzi and A. Zaffaroni, *Comments on the holographic picture of the Randall-Sundrum model*, *JHEP* **04** (2001) 021 [[hep-th/0012248](#)] [[SPIRES](#)].
- [12] M. Pérez-Victoria, *Randall-Sundrum models and the regularized AdS/CFT correspondence*, *JHEP* **05** (2001) 064 [[hep-th/0105048](#)] [[SPIRES](#)].
- [13] R. Contino, Y. Nomura and A. Pomarol, *Higgs as a holographic pseudo-Goldstone boson*, *Nucl. Phys. B* **671** (2003) 148 [[hep-ph/0306259](#)] [[SPIRES](#)].
- [14] K. Agashe, R. Contino and A. Pomarol, *The Minimal Composite Higgs Model*, *Nucl. Phys. B* **719** (2005) 165 [[hep-ph/0412089](#)] [[SPIRES](#)].
- [15] J.M. Maldacena, *The large- N limit of superconformal field theories and supergravity*, *Int. J. Theor. Phys.* **38** (1999) 1113 [*Adv. Theor. Math. Phys.* **2** (1998) 231] [[hep-th/9711200](#)] [[SPIRES](#)].
- [16] S.S. Gubser, I.R. Klebanov and A.M. Polyakov, *Gauge theory correlators from non-critical string theory*, *Phys. Lett. B* **428** (1998) 105 [[hep-th/9802109](#)] [[SPIRES](#)].
- [17] E. Witten, *Anti-de Sitter space and holography*, *Adv. Theor. Math. Phys.* **2** (1998) 253 [[hep-th/9802150](#)] [[SPIRES](#)].
- [18] D.B. Kaplan and H. Georgi, *SU(2) \times U(1) Breaking by Vacuum Misalignment*, *Phys. Lett. B* **136** (1984) 183 [[SPIRES](#)].
- [19] M.J. Dugan, H. Georgi and D.B. Kaplan, *Anatomy of a Composite Higgs Model*, *Nucl. Phys. B* **254** (1985) 299 [[SPIRES](#)].
- [20] G.F. Giudice, C. Grojean, A. Pomarol and R. Rattazzi, *The Strongly-Interacting Light Higgs*, *JHEP* **06** (2007) 045 [[hep-ph/0703164](#)] [[SPIRES](#)].
- [21] R. Contino, T. Kramer, M. Son and R. Sundrum, *Warped/Composite Phenomenology Simplified*, *JHEP* **05** (2007) 074 [[hep-ph/0612180](#)] [[SPIRES](#)].
- [22] M.A. Luty, M. Porrati and R. Rattazzi, *Strong interactions and stability in the DGP model*, *JHEP* **09** (2003) 029 [[hep-th/0303116](#)] [[SPIRES](#)].
- [23] R. Barbieri, A. Pomarol and R. Rattazzi, *Weakly coupled Higgsless theories and precision electroweak tests*, *Phys. Lett. B* **591** (2004) 141 [[hep-ph/0310285](#)] [[SPIRES](#)].
- [24] R. Contino and A. Pomarol, *Holography for fermions*, *JHEP* **11** (2004) 058 [[hep-th/0406257](#)] [[SPIRES](#)].
- [25] G. Panico and A. Wulzer, *Effective Action and Holography in 5D Gauge Theories*, *JHEP* **05** (2007) 060 [[hep-th/0703287](#)] [[SPIRES](#)].
- [26] M.E. Peskin and T. Takeuchi, *Estimation of oblique electroweak corrections*, *Phys. Rev. D* **46** (1992) 381 [[SPIRES](#)].
- [27] R. Barbieri, A. Pomarol, R. Rattazzi and A. Strumia, *Electroweak symmetry breaking after LEP-1 and LEP-2*, *Nucl. Phys. B* **703** (2004) 127 [[hep-ph/0405040](#)] [[SPIRES](#)].
- [28] F. del Aguila et al., *Collider aspects of flavour physics at high Q* , *Eur. Phys. J. C* **57** (2008) 183 [[arXiv:0801.1800](#)] [[SPIRES](#)].

- [29] K. Agashe, A. Delgado, M.J. May and R. Sundrum, *RS1, custodial isospin and precision tests*, *JHEP* **08** (2003) 050 [[hep-ph/0308036](#)] [[SPIRES](#)].
- [30] K. Agashe, R. Contino, L. Da Rold and A. Pomarol, *A custodial symmetry for $Z b$ anti- b* , *Phys. Lett. B* **641** (2006) 62 [[hep-ph/0605341](#)] [[SPIRES](#)].
- [31] M.S. Carena, E. Ponton, J. Santiago and C.E.M. Wagner, *Light Kaluza-Klein states in Randall-Sundrum models with custodial $SU(2)$* , *Nucl. Phys. B* **759** (2006) 202 [[hep-ph/0607106](#)] [[SPIRES](#)].
- [32] M.S. Carena, E. Ponton, J. Santiago and C.E.M. Wagner, *Electroweak constraints on warped models with custodial symmetry*, *Phys. Rev. D* **76** (2007) 035006 [[hep-ph/0701055](#)] [[SPIRES](#)].
- [33] R. Contino, L. Da Rold and A. Pomarol, *Light custodians in natural composite Higgs models*, *Phys. Rev. D* **75** (2007) 055014 [[hep-ph/0612048](#)] [[SPIRES](#)].
- [34] A.D. Medina, N.R. Shah and C.E.M. Wagner, *Gauge-Higgs Unification and Radiative Electroweak Symmetry Breaking in Warped Extra Dimensions*, *Phys. Rev. D* **76** (2007) 095010 [[arXiv:0706.1281](#)] [[SPIRES](#)].
- [35] G. Panico, E. Ponton, J. Santiago and M. Serone, *Dark Matter and Electroweak Symmetry Breaking in Models with Warped Extra Dimensions*, *Phys. Rev. D* **77** (2008) 115012 [[arXiv:0801.1645](#)] [[SPIRES](#)].
- [36] M. Serone, *Holographic Methods and Gauge-Higgs Unification in Flat Extra Dimensions*, *New J. Phys.* **12** (2010) 075013 [[arXiv:0909.5619](#)] [[SPIRES](#)].
- [37] G. Panico, M. Serone and A. Wulzer, *A model of electroweak symmetry breaking from a fifth dimension*, *Nucl. Phys. B* **739** (2006) 186 [[hep-ph/0510373](#)] [[SPIRES](#)].
- [38] G. Panico, M. Serone and A. Wulzer, *Electroweak symmetry breaking and precision tests with a fifth dimension*, *Nucl. Phys. B* **762** (2007) 189 [[hep-ph/0605292](#)] [[SPIRES](#)].
- [39] M.S. Carena, T.M.P. Tait and C.E.M. Wagner, *Branes and orbifolds are opaque*, *Acta Phys. Polon. B* **33** (2002) 2355 [[hep-ph/0207056](#)] [[SPIRES](#)].
- [40] C.A. Scrucca, M. Serone and L. Silvestrini, *Electroweak symmetry breaking and fermion masses from extra dimensions*, *Nucl. Phys. B* **669** (2003) 128 [[hep-ph/0304220](#)] [[SPIRES](#)].
- [41] H. Georgi, A.K. Grant and G. Hailu, *Brane couplings from bulk loops*, *Phys. Lett. B* **506** (2001) 207 [[hep-ph/0012379](#)] [[SPIRES](#)].
- [42] P. Bamert, C.P. Burgess, J.M. Cline, D. London and E. Nardi, *$R(b)$ and new physics: A Comprehensive analysis*, *Phys. Rev. D* **54** (1996) 4275 [[hep-ph/9602438](#)] [[SPIRES](#)].
- [43] G. Altarelli and R. Barbieri, *Vacuum polarization effects of new physics on electroweak processes*, *Phys. Lett. B* **253** (1991) 161 [[SPIRES](#)].
- [44] G. Altarelli, R. Barbieri and S. Jadach, *Toward a model independent analysis of electroweak data*, *Nucl. Phys. B* **369** (1992) 3 [*Erratum ibid.* **B 376** (1992) 444] [[SPIRES](#)].
- [45] G. Altarelli, R. Barbieri and F. Caravaglios, *Nonstandard analysis of electroweak precision data*, *Nucl. Phys. B* **405** (1993) 3 [[SPIRES](#)].
- [46] K. Agashe and R. Contino, *The minimal composite Higgs model and electroweak precision tests*, *Nucl. Phys. B* **742** (2006) 59 [[hep-ph/0510164](#)] [[SPIRES](#)].

- [47] R. Barbieri, B. Bellazzini, V.S. Rychkov and A. Varagnolo, *The Higgs boson from an extended symmetry*, *Phys. Rev. D* **76** (2007) 115008 [[arXiv:0706.0432](#)] [[SPIRES](#)].
- [48] LEP collaboration, *A Combination of preliminary electroweak measurements and constraints on the standard model*, [hep-ex/0412015](#) [[SPIRES](#)].
- [49] ALEPH collaboration, J. Alcaraz et al., *A Combination of preliminary electroweak measurements and constraints on the standard model*, [hep-ex/0612034](#) [[SPIRES](#)].
- [50] C. Anastasiou, E. Furlan and J. Santiago, *Realistic Composite Higgs Models*, *Phys. Rev. D* **79** (2009) 075003 [[arXiv:0901.2117](#)] [[SPIRES](#)].
- [51] TEVATRON ELECTROWEAK WORKING GROUP AND CDF AND D0 collaboration, *Combination of CDF and D0 Results on the Mass of the Top Quark*, [arXiv:0903.2503](#) [[SPIRES](#)].